Forces, Fishes, and Fluids: Hydrodynamic Mechanisms of Aquatic Locomotion

George V. Lauder[1] and Eliot G. Drucker[2]

[1]Museum of Comparative Zoology, Harvard University, Cambridge, Massachusetts 02138; and [2]Department of Ecology and Evolutionary Biology, University of California, Irvine, California 92697

Understanding how fishes generate external fluid force to swim steadily and maneuver has proven to be difficult because water does not provide a stable platform for force measurement. But new methods in experimental fluid mechanics provide insights into the physiological mechanisms of aquatic force generation and limits to locomotor performance.

Comparative physiologists and neurobiologists have long been interested in the mechanisms used by aquatic organisms to propel themselves through water (2, 17). Fishes in particular have served as a model system for understanding the generation of rhythmic locomotor patterns such as undulatory body bending arising from segmental muscle activity. Beginning with the remarkable early work of Erich von Holst (10) and continuing with Sir James Gray's pioneering experimental efforts (9), the field of motor control of rhythmic movements in fishes has expanded greatly and is now a subdiscipline of its own, involving analyses of muscle activation patterns, skeletal movement, and neural circuitry (8, 14, 16).

This focus on the "internal" physiological mechanisms that govern fish locomotion has resulted in a greatly improved understanding of how the musculoskeletal system and neural circuits generate swimming movements, but the mechanisms by which locomotor forces from the body and fins are transmitted to the water externally have remained largely obscure. As a result, we have relatively little knowledge of how movements initiated by the nervous system result in the production of thrust for propelling animals forward and in the generation of directional forces that are necessary for maneuvering.

The difficulty in illuminating mechanisms of aquatic force production can be appreciated by first considering the relative ease with which forces can be measured during locomotion on land. Through the use of force plates mounted on the floor, the forces exerted on the ground by limbs can be directly transduced (1). As each limb contacts the force plate, small deformations of the fixed plate can be measured in the vertical, mediolateral, and anteroposterior directions. By contrast, during aquatic locomotion forces are exerted by the body and fins against the surrounding water, which is not fixed in position but instead yields in response to the action of propulsive surfaces. How then can the magnitude and orientation of applied forces be quantified during aquatic locomotion?

This question is of more than technical interest, as many issues of significant physiological and biomechanical import depend on our ability to measure aquatic forces accurately. To calculate the efficiency of animal propulsion through water, for example, we need to know not just the energy input supplied to fins by the musculature but also the energy output into the fluid. In addition, without the ability to determine the direction of forces exerted on the water by the fins and body, the orientation of reaction forces will remain unknown, as will moments around the center of mass. Finally, the effect of different fin shapes and movement patterns on locomotor function will remain highly inferential until in vivo measurements of aquatic force can be made.

In this article we review a new approach, modified from techniques developed by experimental hydrodynamicists, that we have used to study the external forces exerted by swimming fishes. We first describe how such force measurements are made and then present several key results.

Measuring wake flow patterns

The first step in measuring locomotor forces generated by swimming fishes is to quantify the water flow pattern in the wake of the body and fins. Figure 1 illustrates the experimental arrangement used to accomplish this goal. Fish swim in a recirculating flow tank with water that has been seeded with small (12 μm mean diameter), near-neutrally buoyant, silver-coated, hollow glass beads (4, 11). These silver particles reflect light from a laser that has been focused by a series of optics into a light sheet 1- to 2-mm thick and 10- to 20-cm wide. The light sheet is directed into the flow tank by a mirror and illuminates a slice of the flow within the working area. Figure 1*A* shows a light sheet in vertical orientation (representing the *xy* plane). Fish are trained to swim so that their fins move in or just upstream of the light sheet, and movement of water resulting from fin motions is imaged by a high-speed video camera. The orientation of the light sheet can be altered by changing the positions of mirrors and optics to allow a view of water flow in either the vertical, horizontal, or transverse plane. A second synchronized video camera is used to record the position of the fin or body relative to the light sheet, either through a small mirror placed downstream in the flow tank or from a ventral or lateral perspective.

Pairs of consecutive images from the video sequences are then input into a cross-correlation processing algorithm, which takes a small, user-defined area of the image and calculates the direction and speed of particle motion within that region (20). This yields a single velocity vector representing the average flow within that small area. Continuing such pro-

0886-1714/02 5.00

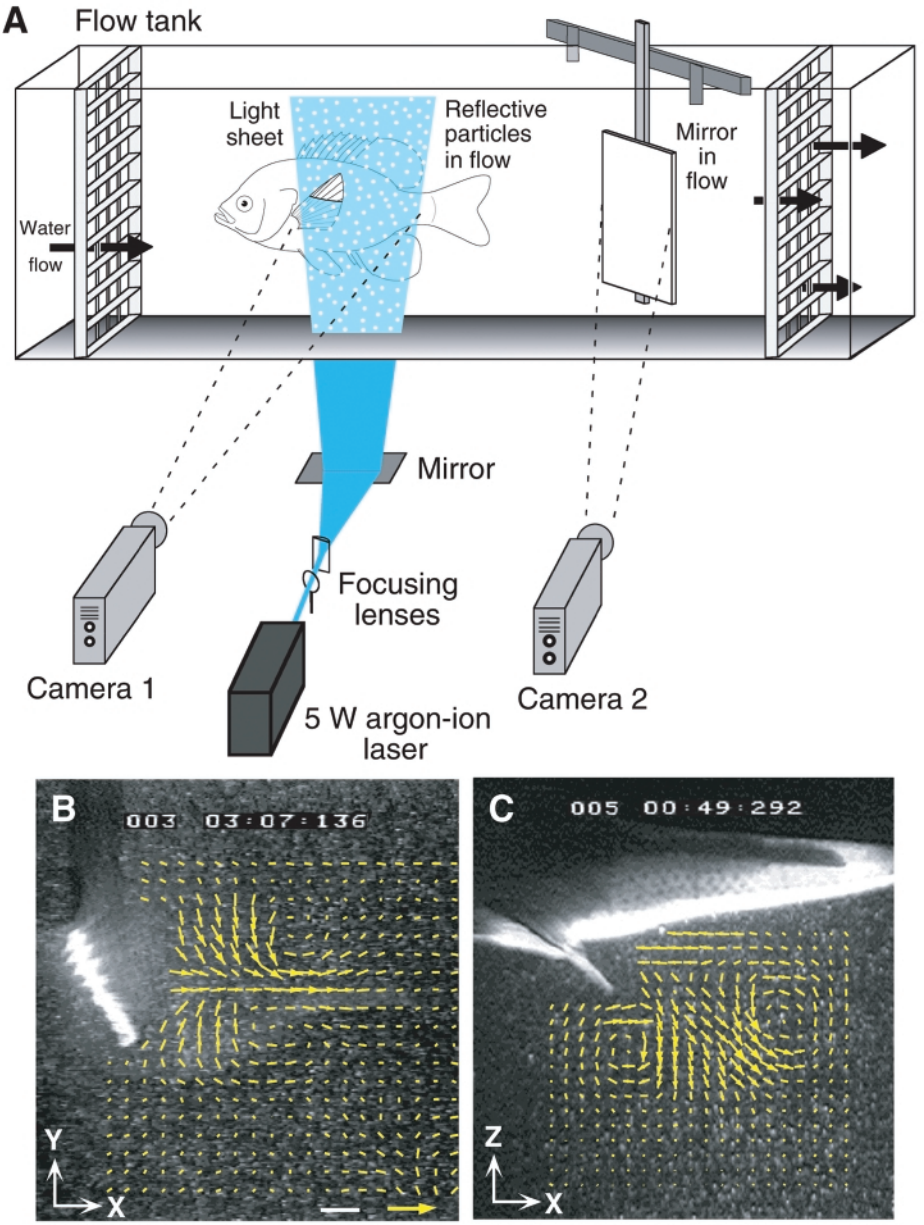

FIGURE 1. Schematic illustration of the technique of digital particle image velocimetry (DPIV) as applied to the study of locomotion in fishes. *A*: fish swim in a recirculating flow tank, and a laser beam is focused into a 1- to 2-mm-thick light sheet, which illuminates a planar section of moving water; a vertical light sheet is illustrated. Fish are trained to swim with their fins moving through this light sheet so that the resulting wake flow patterns can be imaged with a high-speed digital video system (Camera 1). A second camera simultaneously records a perpendicular reference view showing the position of the fins relative to the light sheet. The focusing lenses and mirror can be reoriented to produce a light sheet in different orthogonal planes. *B* and *C*: vertical (*xy*) and horizontal (*xz*) light sheets, respectively, showing the velocity vector fields (yellow arrows) calculated from DPIV images of pectoral fin wake flow. Two counterrotating vortices are visible in each plane, with a central jet of relatively high-velocity flow. Scales for *B* and *C*: bar, 1 cm; arrow, 20 $cm \cdot s^{-1}$.

cessing by stepping across and down the image to cover a larger region of flow within the light sheet behind the fin, and by repeating the cross-correlation analysis at each location, a matrix of velocity vectors can be calculated that provides a snapshot of wake structure and strength (4, 11, 15, 19). This entire procedure is known as digital particle image velocimetry (DPIV) and represents a standard technique in experimental fluid mechanics (18).

Figure 1*B* shows flow within the vertical (*xy*) plane in the wake of the pectoral fin of a bluegill sunfish (*Lepomis macrochirus*) swimming steadily at 0.5 body length $(L) \cdot s^{-1}$. Calculation of the matrix of velocity vectors in the vertical plane reveals a pair of counterrotating vortices with a central high-velocity jet flow directed posteriorly and ventrally. The reaction force arising from this pectoral fin stroke is thus directed forward and upward. In the horizontal (*xz*) plane a similar pattern of vortex flow is seen (Fig. 1*C*). These pairs of counterrotating flow centers seen in orthogonal laser light sheets reflect slices through three-dimensional vortex rings that are shed by the pectoral fins as they beat during swimming. In the case of the bluegill sunfish swimming slowly, each pectoral fin beat produces a single vortex ring that contains a central jet of high-velocity flow oriented ventrally, posteriorly, and laterally (Fig. 2*A*); the wake consists of discrete vortex rings, shed by the pectoral fins on each side of the body, which drift downstream as the sunfish moves forward. DPIV has thus provided insight into a fundamental aspect of aquatic locomotor biomechanics: momentum shed into the fluid by moving fish fins is represented by vortex ring structures.

Calculating locomotor force

Given a matrix of velocity vectors resulting from a fin beat and the determination that fin wakes consist of vortex rings, it

is relatively simple to calculate the time-averaged locomotor force. Total locomotor force is calculated by dividing the fluid momentum of the vortex ring (or rings) shed over a fin beat cycle by the duration of the fin beat. The momentum of each vortex ring is itself calculated as the product of the density of water, the area of the vortex ring, and mean ring circulation (3, 4). Circulation measures vortex strength and is taken as the line integral of velocity tangential to a closed path around the vortex center. Total force is geometrically resolved into *x*, *y*, and *z* components according to the average orientation of the central wake momentum jet measured from DPIV vector matrices. Thrust is that component of force in the *x* direction, lift force is the *y* component, and mediolateral force is oriented in the *z* direction (cf. Fig. 1, *B* and *C*).

For bluegill sunfish swimming at 0.5 $L \cdot s^{-1}$ with the pectoral fins, each fin generates 5 mN thrust force, 2 mN lift, and 7 mN lateral force over the course of the stroke (Fig. 2*A*). We were surprised to find that laterally oriented force exceeds thrust force during pectoral fin locomotion, but we obtained a similar result during analyses of the tail wake in sunfish. At 1.5 $L \cdot s^{-1}$ the caudal fin generates a set of linked vortex rings in the wake, each of which produces 14 mN of thrust and 23 mN of lateral force (Fig. 2*C*). These relatively high lateral forces have also been measured during caudal fin locomotion in mackerel (*Scomber japonicus*), a species within the high-performance scombrid clade of fishes that includes the bonitos and tunas (15), and they appear to be a general feature of undulatory propulsor function in fishes.

Experimental validation of the DPIV force calculations was conducted by measuring total drag force on fishes towed in

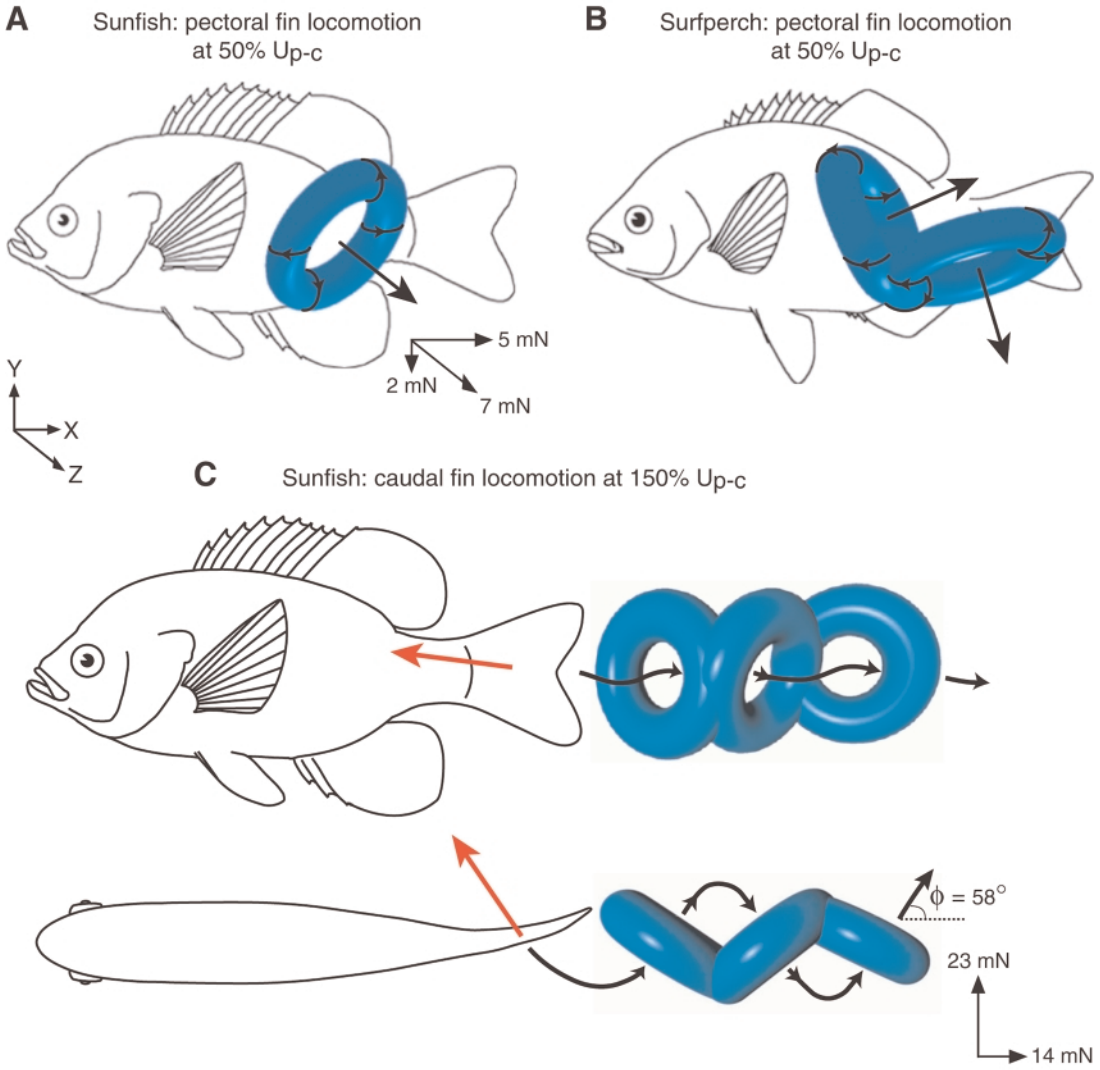

FIGURE 2. Vortex wakes of swimming fishes. Vortex generation is a hallmark of fluid force production, and fish fins shed vortex rings into the wake during locomotion. *A* and *B*: bluegill sunfish and black surfperch swimming at 50% of their maximal pectoral fin swimming speed; curved arrows represent vortices observed in vertical and horizontal laser light sheets. These species shed wakes consisting, respectively, of discrete vortex rings and linked vortex rings, each with central high-velocity jet flow (large black arrows). Average wake force components calculated from DPIV data for the left pectoral fin of sunfish are shown in *A*. *C*: lateral and dorsal views of sunfish swimming with the caudal fin that generates a chain of linked vortex rings in the wake (curved arrows represent central jet flow). ϕ indicates the mean jet angle measured relative to the path of motion; lateral and thrust forces calculated from the tail wake (per vortex ring) are shown at *right*. The total reaction force exerted on the tail is represented by red arrows. $U_{p\text{-}c}$, gait transition speed from pectoral-to-caudal fin locomotion.

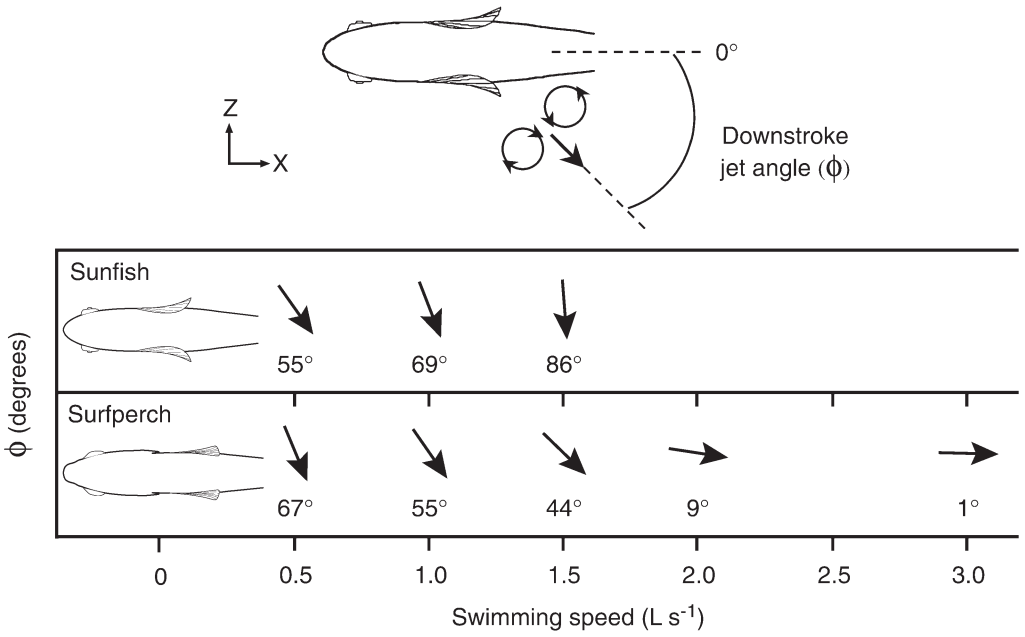

FIGURE 3. Pectoral fin vortex ring jet orientation in sunfish and surfperch as a function of swimming speed. In sunfish, the momentum jet becomes progressively more laterally directed as speed increases, resulting in decreased thrust and the necessary recruitment of additional propulsive fins to overcome drag (above 1.0 $L{\cdot}s^{-1}$, the dorsal and caudal fins are recruited to supplement pectoral fin force). In contrast, the vortex ring jet of surfperch reorients increasingly downstream as speed increases (up to and above the maximum pectoral-fin swimming speed of 2.0 $L{\cdot}s^{-1}$), enhancing thrust. Such differences in wake jet orientation may underlie interspecific variation in the upper limit to swimming speed.

the flow tank; empirically determined body drag is not statistically different from the thrust force calculated from DPIV data (4, 15).

Wake structure shows interspecific variation

Although the generation of vortex rings by swimming fishes is a hallmark of fluid force production, species differ considerably in the morphology of these wake structures. At the same relative speed of locomotion (half of maximal pectoral fin swimming speed), black surfperch (*Embiotoca jacksoni*) generate a linked pair of vortex rings with each pectoral fin beat (Fig. 2*B*), in contrast to the single ring produced by bluegill sunfish (Fig. 2*A*). Unlike sunfish, which shed one ring over the duration of the entire fin stroke cycle, surfperch generate a separate ring on the downstroke, form a link between rings as the fin switches to the upstroke, and complete a second, upstroke ring at the end of the fin beat (5). Perciform fishes swimming with the caudal fin generate a linked chain of vortex rings, with each ring produced during one half tail beat (12, 15). Other fishes that swim by oscillating their caudal fin such as sturgeon and sharks also generate linked vortex rings, but these rings may be oriented at a much more oblique angle to the horizontal axis (12, 13). Such differences in wake structure provide critical information for interpreting interspecific variation in swimming performance.

Vortex wake structure may explain maximal locomotor performance

One intriguing result that emerges from interspecific comparisons of wake dynamics is a hydrodynamic explanation of maximal locomotor performance. Limits to swimming performance (i.e., top swimming speed) are often framed in terms of maximal twitch frequency of locomotor musculature or the capacity for muscle power output. But if vortex rings shed into the wake are not oriented appropriately to produce thrust, no amount of muscular power increase to the fin will increase propulsive force and hence speed. Such a constraint appears to be in effect for bluegill sunfish swimming at high speeds (Fig. 3). As sunfish increase pectoral fin swimming speed, the vortex rings reorient progressively more to the side until the central momentum jet is directed nearly laterally at the maximum pectoral swimming speed of 1.0 $L{\cdot}s^{-1}$. With a lateral momentum jet at this highest sustainable pectoral fin swimming speed, any further increase in mechanical power to the fin will result in a negligible increase in thrust. Sunfish are able to swim faster only by recruiting other fins to supplement thrust forces generated by the pectoral fins. In surfperch, which can swim twice as fast as sunfish with the pectoral fins alone, vortex rings reorient increasingly downstream with increasing speed (Fig. 3) so that jet momentum, and associated thrust force, is augmented. We conclude that swimming performance, as measured by maximal swimming speed within a gait, may be limited by a species' ability to direct wake momentum downstream.

Multiple fin control surfaces permit versatility in force production

One of the most striking aspects of fish diversity is the presence of multiple locomotor control surfaces. Almost all fishes have (minimally) a caudal fin, one or more dorsal fins, paired pectoral and pelvic fins, and an anal fin. The hydrodynamic roles of these different fins during steady swimming and during unsteady maneuvering locomotion, as well as the possi-

bility of vortex wake interactions among fins, are just beginning to come under study (6, 7, 13, 19).

The impressive functional versatility of fish fins is revealed through a comparison of fin kinematics and wake dynamics during steady swimming and turning. Bluegill sunfish swimming steadily at 1.1 $L \cdot s^{-1}$ recruit the pectoral fins, caudal fin, and dorsal fin simultaneously in bilaterally symmetrical strokes to generate thrust sufficient to overcome drag (Fig. 4*A*). During slow turning, the pectoral and dorsal fins are also recruited but act unilaterally to generate rotational moments around the center of mass. The proportion of total force exerted by each pectoral fin is considerably higher during turning (Fig. 4*B*) than during straight-ahead swimming (Fig. 4*A*). In sunfish, yawing turns are accomplished by rapid abduction of the strong-side pectoral fin (i.e., the fin nearer the turning stimulus), which generates a laterally directed momentum jet to rotate the fish away from this stimulus (Fig. 4*C*). Body rotation is followed by adduction of the weak-side pectoral fin, which generates posteriorly directed thrust force, translating the fish away from the stimulus (Fig. 4*D*). Left- and right-side fins therefore are capable of serving quite different functions during maneuvering.

Adjacent fins may, in addition, act in concert to augment thrust. Experimental study of the wake of the dorsal fin shows that shed vortices are intercepted by the tail in a manner that is consistent with reinforcement of bound tail vorticity. Such vorticity enhancement is a possible mechanism for increasing overall thrust production by the caudal propeller (6).

Prospectus

The ability to quantify the wake of swimming fishes by measuring velocity vector fields through time allows both the magnitude and orientation of forces exerted on the water to be calculated. As a result, we can now test long-standing hypotheses about the efficiency of swimming and the functional significance of different fin shapes and positions, and in this way we can clarify the hydrodynamic mechanisms of aquatic animal propulsion. Measurement of in vivo locomotor forces promises to allow the study of aquatic propulsion to proceed in a manner comparable with analyses of terrestrial locomotion, for which the direct measurement of propulsive forces has long been an essential tool for the study of mechanics and energetics. In the future, a combination of computa-

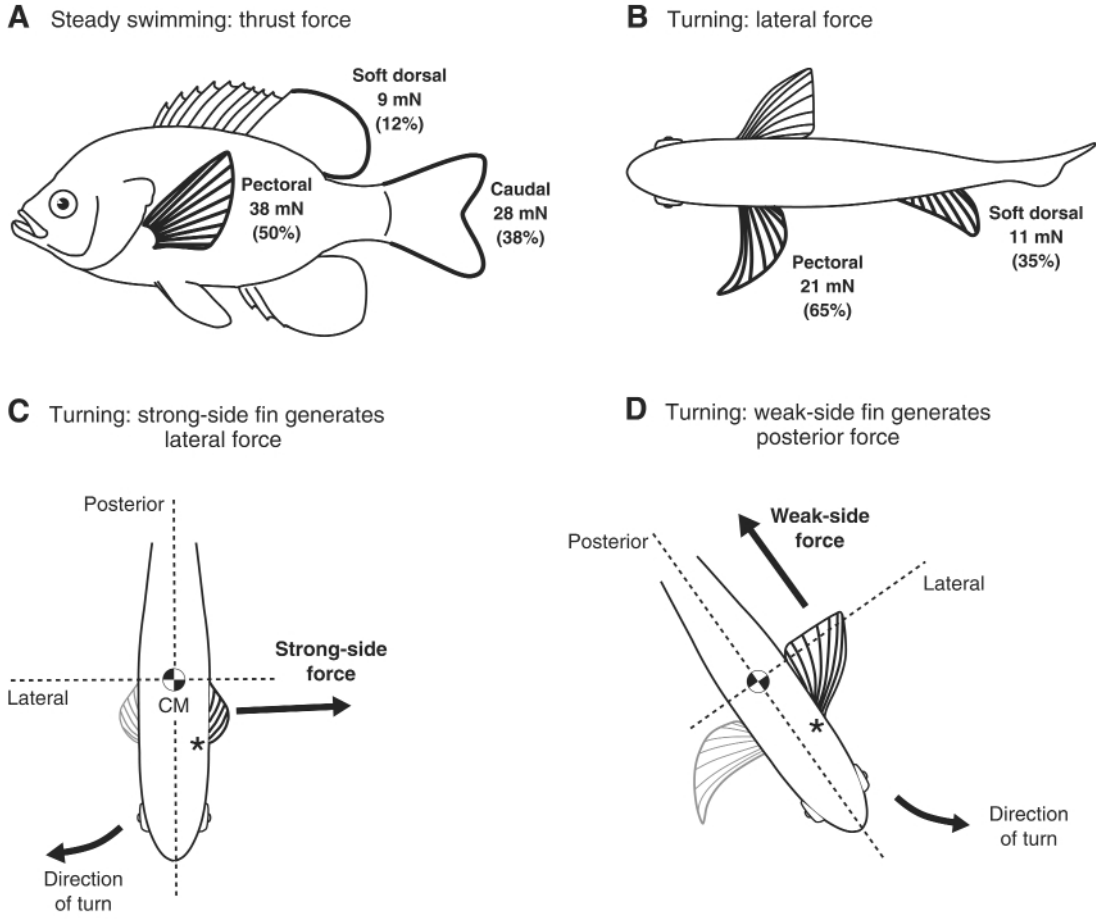

FIGURE 4. Fish fins exhibit considerable hydrodynamic versatility. *A*: at steady swimming speeds over 1.0 $L \cdot s^{-1}$, bluegill sunfish of adult size recruit multiple fins to generate thrust, which is partitioned among the dorsal, pectoral, and caudal fins. *B*: during slow turning, total lateral force is partitioned between the strong-side pectoral fin (closer to the turning stimulus) and the dorsal fin. *C* and *D*: the hydrodynamic role of the pectoral fins on each side of the body differs during turning. The strong-side fin generates lateral force to rotate the head away from the stimulus, while the weak-side fin generates posteriorly directed thrust force to cause body translation. Active fins in each panel are shown in darker outline; asterisk indicates the attachment point of the pectoral fin to the body. CM, center of mass.

tional approaches for estimating flow over deforming surfaces, direct measurement of locomotor forces with robotic fish, and experimental analyses of flow around and in the wake of biological propulsors will lead to a comprehensive understanding of animal movement through water.

This research was supported by National Science Foundation Grants IBN-9807012 (to G. V. Lauder) and IBN-0090896 (to E. G. Drucker and G. V. Lauder).

References

1. Cavagna GA. Force platforms as ergometers. *J Appl Physiol* 39: 174–179, 1975.
2. Cohen AH, Rossignol S, and Grillner S., editors. *Neural Control of Rhythmic Movements in Vertebrates*. New York: John Wiley, 1988.
3. Dickinson MH. Unsteady mechanisms of force generation in aquatic and aerial locomotion. *Am Zool* 36: 537–554, 1996.
4. Drucker EG and Lauder GV. Locomotor forces on a swimming fish: three-dimensional vortex wake dynamics quantified using digital particle image velocimetry. *J Exp Biol* 202: 2393–2412, 1999.
5. Drucker EG and Lauder GV. A hydrodynamic analysis of fish swimming speed: wake structure and locomotor force in slow and fast labriform swimmers. *J Exp Biol* 203: 2379–2393, 2000.
6. Drucker EG and Lauder GV. Locomotor function of the dorsal fin in teleost fishes: experimental analysis of wake forces in sunfish. *J Exp Biol* 204: 2943–2958, 2001.
7. Drucker EG and Lauder GV. Wake dynamics and fluid forces of turning maneuvers in sunfish. *J Exp Biol* 204: 431–442, 2001.
8. Fetcho JR. A review of the organization and evolution of motoneurons innervating the axial musculature of vertebrates. *Brain Res Rev* 12: 243–280, 1987.
9. Gray J. Studies in animal locomotion. II. The relationship between waves of muscular contraction and the propulsive mechanism of the eel. *J Exp Biol* 10: 386–390, 1933.
10. Holst E von. Relative coordination as a phenomenon and as a method of analysis of central nervous functions. In: *The Behavioral Physiology of Animals and Man: Selected Papers of Erich von Holst*, edited by Holst E von. Coral Gables: Univ. of Miami Press, 1973, pp. 33–135.
11. Lauder GV. Function of the caudal fin during locomotion in fishes: kinematics, flow visualization, and evolutionary patterns. *Am Zool* 40: 101–122, 2000.
12. Lauder GV, Drucker EG, Nauen J, and Wilga CD. Experimental hydrodynamics and evolution: caudal fin locomotion in fishes. In: *Vertebrate Biomechanics and Evolution*, edited by Bels V, Gasc J-P, and Casinos A. Oxford, UK: BIOS Scientific. In press.
13. Liao J and Lauder GV. Function of the heterocercal tail in white sturgeon: flow visualization during steady swimming and vertical maneuvering. *J Exp Biol* 203: 3585–3594, 2000.
14. Matsushima T and Grillner S. Neural mechanisms of intersegmental coordination in lamprey: local excitability changes modify the phase coupling along the spinal cord. *J Neurophysiol* 67: 373–388, 1992.
15. Nauen JC and Lauder GV. Hydrodynamics of caudal fin locomotion by chub mackerel *Scomber japonicus*. *J Exp Biol* 205: 1709–1724, 2002.
16. Rome LC, Swank D, and Corda D. How fish power swimming. *Science* 261: 340–343, 1993.
17. Schmidt-Nielsen K. *Animal Physiology: Adaptation and Environment*. London: Cambridge Univ. Press, 1975.
18. Stanislas M, Kompenhans J, and Westerweel J, editors. *Particle Image Velocimetry: Progress Toward Industrial Application*. Dordrecht, The Netherlands: Kluwer Academic, 2000.
19. Wilga CD and Lauder GV. Three-dimensional kinematics and wake structure of the pectoral fins during locomotion in leopard sharks *Triakis semifasciata*. *J Exp Biol* 203: 2261–2278, 2000.
20. Willert CE and Gharib M. Digital particle image velocimetry. *Exp Fluids* 10: 181–193, 1991.